Molecular Crystals and Liquid Crystals
Publication details, including instructions for authors and subscription information:
http://www.tandfonline.com/loi/gmcl20

Apertureless SNOM Microscopy on a Commercial AFM

Giovanni Carbone [a], Bruno Zappone [a], Riccardo Barberi [a] & Roberto Bartolino [a]

[a] Istituto Nazionale di Fisica della Materia - Unità di Ricerca della Calabria - Dipartimento di Fisica, Università degli Studi della Calabria, Rende (CS), 87036, Italia

Version of record first published: 29 Oct 2010

To cite this article: Giovanni Carbone, Bruno Zappone, Riccardo Barberi & Roberto Bartolino (2002): Apertureless SNOM Microscopy on a Commercial AFM, Molecular Crystals and Liquid Crystals, 372:1, 373-382

To link to this article: http://dx.doi.org/10.1080/10587250127578

Mol. Cryst. and Liq. Cryst., 2001, Vol. 372, pp. 373-382

Apertureless SNOM Microscopy on a Commercial AFM

GIOVANNI CARBONE, BRUNO ZAPPONE, RICCARDO BARBERI and ROBERTO BARTOLINO

Istituto Nazionale di Fisica della Materia - Unità di Ricerca della Calabria - Dipartimento di Fisica - Università degli Studi della Calabria - 87036 -Rende (CS) - Italia

Abstract: We have implemented an apertureless Scanning Near-Field Optical Microscope (SNOM) setup on a commercial Atomic Force Microscope (AFM), using a suitable optical apparatus and preserving AFM performances. This approach is promising for extending SNOM analysis to delicate samples, such as liquid or polymer films. Preliminary measurements on glass-metal nanometric steps show a lateral resolution better than 10 nm both in topography and in optical signal.

Keywords: AFM, SNOM, SPM

INTRODUCTION

Scanning Probe Microscopes (SPM) such as Atomic Force Microscope (AFM) have provided a great insight in surface physics, allowing direct measurement of a wide range of surface properties (f.i. topography, mechanical properties, static conductivity, magnetic permeability) with a typical lateral resolution of 10 nm [1]. Yet, being based on the measure of the interaction strength between a probe and the sample, they are unable to provide information about optical properties of surfaces, such as dielectric constant, conductivity at optical frequencies or chemical composition.

The SNOM (Scanning Near-field Optical Microscope) overrides this limitation directly measuring the light produced or scattered by the surface in the near-field, i.e. on a scale much smaller than the wavelength [2].

Working in the near field is necessary in order to achieve the typical SPM lateral resolution. In fact, as the diffraction analysis shows, all devices measuring light intensities in the far-field, and in particular the traditional optical microscopes, are limited in the visible region to a resolution of about 200 nm, given by the Abbe's formula [3]. The reason is that any sub-wavelength superficial distribution of optical properties produces evanescent waves, that propagate parallel to the surface and decay exponentially with the distance from the surface, thus being unable to reach light detectors placed in the far field [2,4].

At present, there are two main different SNOM setups: the aperture and the apertureless SNOM. The aperture setup uses a thin metal-covered optical fiber to illuminate nanometric regions of the surface or to pick up the local optical response [5, 6, 7]. The lateral resolution is limited to about 15 nm by the skin depth of the light field in the covering metal [7, 8]. The apertureless setup uses a thin metallic or dielectric tip, that spreads the local near field from the surface to the optical instrumentation placed in the far field [8, 9, 10]. The resolution is mainly determined by the size of tip end, which can be as small as a few nanometers.

We have realized an apertureless SNOM setup on a pre-existent commercial AFM working in Non-Contact or Intermittent-Contact mode, because commercial AFMs guarantee good stability and high precision in topographic measurement. This is a crucial problem in SNOM microscopy for three reasons. First, a good tip-sample distance control prevents the tip from being damaged by mechanical contact with the surface. Second, unwanted deviations of the tip trajectory in the near field may alter SNOM images, because even small variations in the evanescent field produce significant variations of the diffused signal. Third, theoretical studies [11] show that different surface properties influencing scattered intensity (specially topography and local refractive index) play an equivalent role in forming the scattered waves and hence different surfaces can have the same SNOM image. It is therefore necessary to compare the SNOM images with the topographical ones to underline the features of the near field that are not due to the topography.

REALIZATION OF THE SNOM SET-UP

We have chosen to build the SNOM setup without modifying any components of the pre-existent commercial AFM. The AFM part is a ThermoMicroscopes Autoprobe-CP, working in Non-Contact or Intermittent-Contact mode (Fig. 1a) and using 10-15 μm long silicon tips, manufactured on a rectangular cantilever.
Preserving the performances of the AFM part, in principle, allows to extend the field of application of SNOM to the wider field of commercial AFM's. SNOM setups are in general limited by tip sample distance control, which is low-engineered for most home-made SNOM and not yet well understood for aperture SNOM, that perform horizontal oscillation of the optical fiber ("shear-force" [2, 12, 13]).

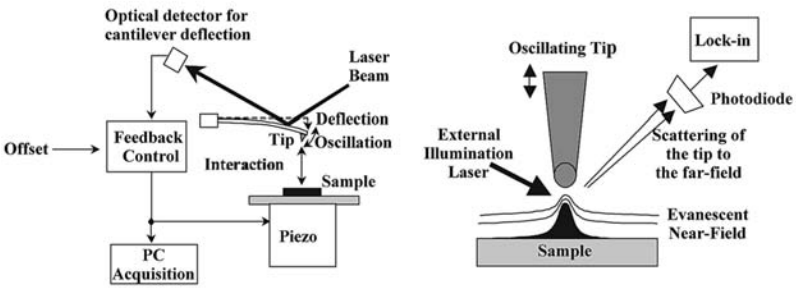

FIG.1: Scheme for Non-Contact or Intermittent-Contact AFM (a) and Apertureless SNOM (b).

The apertureless SNOM is based upon Non-Contact or Intermittent Contact AFM, whose general scheme is depicted in Fig. 1a. The AFM tip-distance control keeps a fixed tip oscillation by moving vertically the sample, mounted on a piezoelectric ceramic. The amplitude variation (error signal) is recorded. It will be useful for distinguishing artifacts from true optical effects in the SNOM images.

To obtain the SNOM signal, an external laser beam is focused on the surface (Fig. 1b) into a spot of about 50x30 μm², in the tip/sample interaction zone (see c Fig. 2). The light spot is large enough to contain the full tip. Hence laser illumination behaves like a planar wave impinging on the interaction area.
The tip oscillates in the illuminated region, where sub-wavelength surface details produce local evanescent near field. SNOM signal is created when the tip scatters this evanescent near-field towards far field optical detectors.

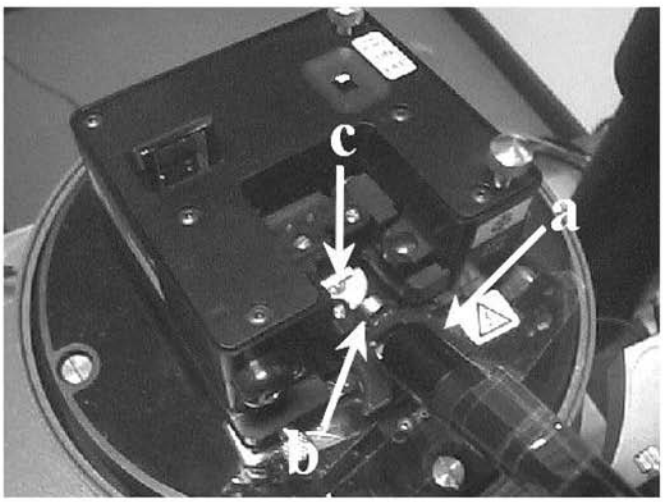

FIG.2: ThermoMicroscopes Autoprobe-CP AFM head. (a) External illumination laser (b) SNOM detection photodiode. (c) Tip/sample interaction zone.

Both illumination and detection optics are kept as small as possible, in order to be more easily adaptable to commercial AFM heads, which usually offer only a small solid angle for illumination and detection (Fig. 2).
The illumination system (see a in Fig.2) is a laser diode with a wavelength λ≅660nm and an optical power of about 5 mW. A small

suitable in-axis optics focuses the laser beam into a spot of about 50x30 μm^2. This choice allows us to get a good energy density in the interaction tip-sample zone and an efficient position control of the spot on the sample surface.

The detection system is based on a small silicon photodiode (see b in figure 2), whose active surface is about 13 mm^2, set at a distance of 1 cm from the tip, that provides a solid angle of 0.13 sterads for light detection.

The scattered light detected in far field is composed by two parts: the background scattered by the sample surface (low resolution signal) and the SNOM response, which is the light modulated by the tip moving in the near-field.

The SNOM signal is extracted by means of a lock-in referenced at the oscillation frequency of the AFM tip.

During the scan, the standard I/O AFM system records topographical and error signals and a dedicated external I/O module allows to simultaneously record other analogical external signals in the range from -10 to +10 Volt. We use this module for recording the signal extracted by the Lock-in.

These signals are treated by the acquisition software on a PC by allowing the simultaneous drawing of both the topographical and SNOM images.

EXPERIMENTAL SNOM IMAGES

To start to check the efficiency of the SNOM setup we have realized an home-made test sample: a gold step of about 50 nm evaporated on a plane glass substrate. Figure 3 shows the AFM and the SNOM images obtained in air by external reflection. The laser beam is *p*-polarized by a polaroid and it is parallel to the arrow on figure 3, forming an angle of about 30° with the substrate.

The SNOM image shows a modulation in the optical signal, running parallel to the glass/gold border line and extending several wavelengths away from it, where topography is completely flat.

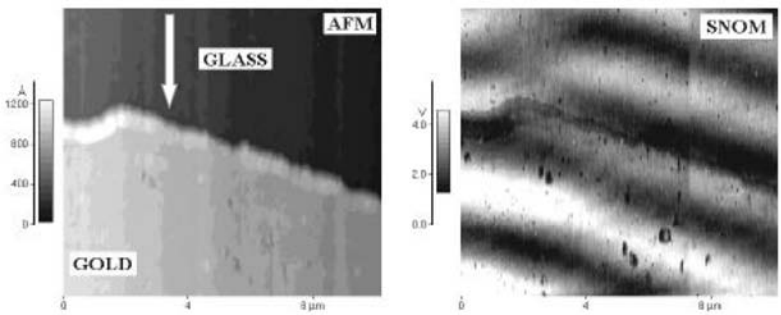

FIG.3: 10 x 10 μm^2 (a) AFM and (b) SNOM image of a gold step on a glass substrate

The appearance of such modulation is due to the interference between the waves diffracted by the gold-glass edge and the incident laser beam, but one can hardly account of all the features of this figure using simple geometrical models in simulations. For instance, Sommerfeld's sharp discontinuity for a conducting half-plane will lead to much shorter modulations and to a sharp intensity peak at the discontinuity [3], detected in other experiment [14].

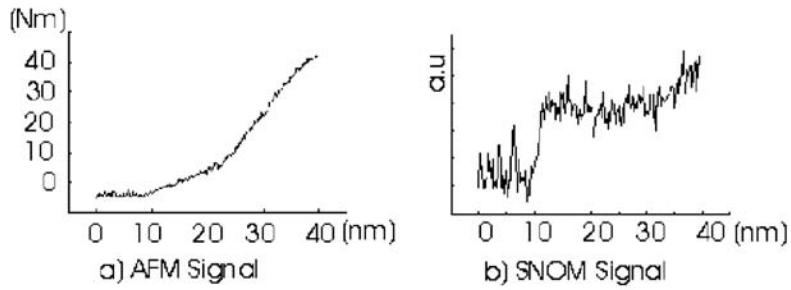

FIG.4: (a) AFM and (b) SNOM signal of a scan performed on the same sample of FIGURE 2. The scan is performed on 40 nm

The real geometry of the gold-glass edge on a nanometric scale is quite complicated, as shown in figure 4a, where the AFM scans a 40 nm line across the gold step. Observing the topographical image, one can deduce that in the 0-10 nm region the tip is moving on the glass substrate, at about 10 nm from the beginning of the scan the gold layer joins the substrate with a mean angle $\alpha \cong 50°$ with respect to the horizontal plane and the SNOM signal (Fig. 4b) begins to grow very quickly. The topography continues to grow in the 10-40 nm region, but SNOM signal achieves the maximum amplitude at the position 15 nm and then it is practically constant.

The observed different resolution between these SNOM and AFM scans is a first signal of the SNOM nature of optical acquisition [15] and shows the high sensitivity of the SNOM setup.

We also analyzed a 120 nm chromium layer joining a plane glass substrate (Fig. 5) with an angle larger than 50° with respect to the horizontal plane and with the same illumination condition used for the gold step sample. In this case, we performed an error signal analysis. It shows that the vibration amplitude of the tip is quite constant during all the acquisition and it is not correlated with the SNOM signal. We note that the amplitude of the optical response is higher on the chromium than on glass, because of the higher reflectivity of the metal.

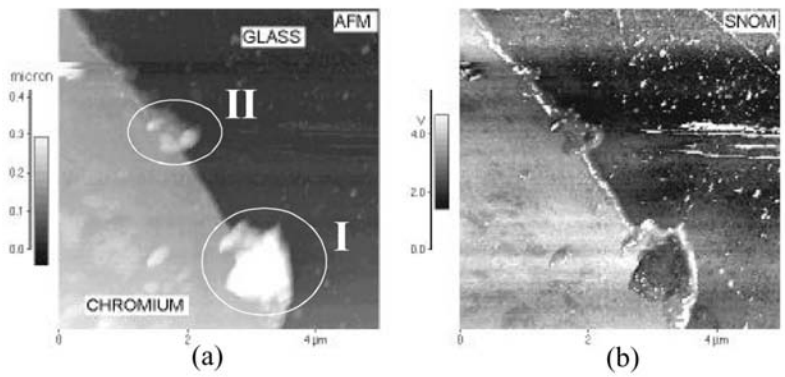

FIG.5: 5 x 5 μm^2 (a) AFM and (b) SNOM image of a chromium step on a glass substrate

Moreover, the topography shows a bump on the chromium layer close to the chromium-glass border (I in Fig. 5a) , that corresponds to an attenuation in the optical signal. This could be due to the different sample composition in this point. The bump has not the same optical response of chromium: it could be a dust particle. Unfortunately, this interpretation is not unique. In fact similar optical responses could be due to the variation of the z position of the tip [15].
We just remark also that a similar feature is present for the smaller bump in the upper part of the picture along the chromium-glass border (II in Fig.5a), where the tip z-position is comparable with the height of the chromium step itself. Hence the SNOM signal seems to be responsible of all details of the picture reported in Fig. 5b.

CONCLUSIONS

We have implemented a SNOM setup on a commercial AFM, without any modification of the AFM part, using a compact optical apparatus. The setup has succeeded in imaging optical field scattered by metal-dielectric surface, but a better characterization of optical signal is at present required.

As previously mentioned, the ambiguity in the interpretation of the optical image is introduced by the topography of the sample surface.

To minimize undesired effect due to the tip z-motion, it is suitable a higher selectivity in the demodulation of the acquired optical signal. This is possible using a second harmonic lock-in demodulation of the signal provided by the photodiode [16]. First attempt failed due to the low level of this signal.

Moreover, it is suiteble the use of samples with flat surface. The study of a flat sample allows the tip to oscillate in a plane in which far field has quite constant amplitude and phase, while near field is affected by local chemical disomogeneities. This gives an unambiguous interpretation of optical signals. The second possibility is the use of a Total Internal Reflection (TIR) to illuminate the sample surface. In this configuration no propagating waves are present in the tip sample interaction zone and z-motion has not undesired consequences.

Exploiting the reliability and precision of commercial AFM in controlling probe/sample distance, we hope to apply SNOM analysis to delicate samples, like liquid crystals or polymer films, recently imaged by Non-Contact AFM [17]. A good example of possible applications is the study of the precursors layer in liquid films.

The precursor is usually a monolayer with the thickness comparable to the molecular size. Only very sensible AFMs can be used to image it. SNOM revelation can extract deeper information on its structure.

ACKNOWLEDGMENTS

We thank A. C. Boccara and J. C. Rivoal at the ESPCI-Paris for collaboration in the realization of the SNOM setup and L. Blinov for providing us the chromium test sample.

REFERENCE

[1] D. Sarid, "Scanning Force Microscopy", Oxford University Press (1994) **56**,9,(1986),930.

[2] D. Courjon, D. Bainier, Rep. Prog. Phys., **57**, (1994), 989

[3] M. Born, E. Wolf, Principles of Optics, Cambridge (1980)

[4] E. Wolf, M. Nieto-Vesperinas, J. Opt. Soc. Am. **2**, (1985),886

[5] U. Durig, D.W. Pohl, H. Rohner, J. Appl. Phys., **59,** (1986), 3318

[6] E. Betzig, A. Harootunian, M. Isaacson, E. Kratschmer, Biophys. J., **49** (1986), 296

[7] D. Courjon, K. Sarayeddine, M. Spajer, Opt. Comm., **71** (1989)

[8] F. Zenhausern, M.P. O'Boyle, and H.K. Wickramasinghe, Appl. Phys. Lett. **65**, 1623 (1994)

[9] R. Bachelot, P. Gleyzes, A.C. Boccara, Appl Opt., **36**,10, (1997), 2160

[10] P. Gleyzes, A. C. Boccara, R. Bachelot, Ultramicroscopy, **57** (1994), 318

[11] R. Carminati, J. -J. Greffet, J. Opt. Soc. Am., **12**, (1995), 2716

[12] E. Betzig, P. L. Finn, and J.S. Weiner, Appl. Phys. Lett., **60** (20), 1992, 2484

[13] J-K Leong, and C. C. Williams, Appl. Phys. Lett. , **66** (11), 1995, 1432

[14] S. Gresillon, H. Cory, J. C. Rivoal, A. C. Boccara, Journal of Optics A, **2** (1999)

[15] B. Hecht, H.Bielefeldt, Y. Inouye, D.W. Pohl, and L.Novotny, J. Appl. Phys 81, 2492 (1997)

[16] M. Labardi, S. Patanè, M. Allegrini Appl. Phys. Lett. , **77** (5), 2000, 621.

[17] L.Xu, M.Salmeron, S. Bardon, Phys. Rev. Lett., **84 (7) ,** 2000, 1519.